the plasma becomes embedded. A typical dissipation time is 0.5 msec. Since this is short compared to the inferred impact frequency, the phenomenon is dominated by single events. The step-function increases in voltage associated with the production of charged plasma exhibit an f^{-2} flux density spectrum; however, such a spectrum is modified at low frequencies by the impact rate itself and at high frequencies by dissipation effects and plasma physical phenomena. Additional modifications could result from spacecraft interactions with the plasma. Therefore, an impact discharge phenomenon could produce a spectrum like that shown in Fig. 6.

In this model, the Voyager 2 PRA and plasma wave science instruments act in tandem to yield in situ measurements of G ring material. The falloff in intensity and the change in spectrum away from the ring plane are attributed to variations in particle size and number density along the path of the spacecraft. The total vertical thickness of ~ 1500 km inferred from the duration of the ring plane noise event is much greater than the optical thickness reported for any of Saturn's major rings. Hence, these data indicate that the G ring possesses a tenuous halo that extends well beyond the nominal ring particle layer—much like the E ring with its 1800-km inferred thickness (*18*).

J. W. WARWICK
D. R. EVANS, J. H. ROMIG
Radiophysics, Inc.,
Boulder, Colorado 80301
J. K. ALEXANDER
M. D. DESCH, M. L. KAISER
Laboratory for Extraterrestrial Physics,
Goddard Space Flight Center,
Greenbelt, Maryland 20771
M. AUBIER, Y. LEBLANC
A. LECACHEUX, B. M. PEDERSEN
Observatoire de Paris,
Section d'Astrophysique de Meudon,
92190 Meudon, France

References and Notes

1. The PRA instrument has a pair of orthogonal, 10-m, monopole antennas and a 198-channel step-frequency receiver to measure the intensity and circular polarization of radio signals between 1.2 kHz and 40.5 MHz [see J. W. Warwick *et al.*, *Space Sci. Rev.* **21**, 309 (1977)].
2. J. W. Warwick *et al.*, *Science* **212**, 239 (1981).
3. D. R. Evans, J. W. Warwick, J. B. Pearce, T. D. Carr, J. J. Schauble, *Nature (London)* **292**, 716 (1981).
4. M. L. Kaiser, M. D. Desch, J. W. Warwick, J. B. Pearce, *Science* **209**, 1238 (1980).
5. M. D. Desch and M. L. Kaiser, *Geophys. Res. Lett.* **8**, 253 (1981).
6. M. L. Kaiser, M. D. Desch, A. Lecacheux, *Nature (London)* **292**, 731 (1981).
7. M. D. Desch and M. L. Kaiser, *ibid.*, p. 739.
8. M. L. Kaiser and M. D. Desch, *Geophys. Res. Lett.* **7**, 389 (1980).
9. H. S. Bridge *et al.*, *Science* **215**, 563 (1982).
10. D. A. Gurnett, W. S. Kurth, F. L. Scarf, *Nature (London)* **292**, 733 (1981).
11. N. F. Ness *et al.*, *Science* **215**, 558 (1982).
12. F. L. Scarf *et al.*, *Nature (London)* **292**, 585 (1981).
13. W. S. Kurth, D. A. Gurnett, F. L. Scarf, *ibid.*, p. 742.
14. F. L. Scarf *et al.*, *Science* **215**, 587 (1982).
15. B. M. Pedersen *et al.*, *Nature (London)* **292**, 714 (1981).
16. R. J. Terrile, private communication.
17. R. N. Clark, *Icarus* **44**, 388 (1980).
18. D. H. Humes, R. L. O'Neal, W. H. Kinard, J. M. Alvarez, *Science* **207**, 443 (1980).
19. We thank R. Holtzman and his staff at the Jet Propulsion Laboratory for computer support during the encounter period and R. Elson and B. Razzaghinejad for computer support throughout the mission. We also thank the other members of the PRA team, especially R. L. Poynter, for their support. The PWS, PLS, and MAG teams provided invaluable information. Our French investigators acknowledge support by Centre National d'Etudes Spatiales. Supported in part by NASA contract NAS 7-100.

10 November 1981

Voyager 2 Plasma Wave Observations at Saturn

Abstract. *The first inbound Voyager 2 crossing of Saturn's bow shock [at 31.7 Saturn radii (R_S), near local noon] and the last outbound crossing (at 87.4 R_S, near local dawn) had similar plasma wave signatures. However, many other aspects of the plasma wave measurements differed considerably during the inbound and outbound passes, suggesting the presence of effects associated with significant north-south or noon-dawn asymmetries, or temporal variations. Within Saturn's magnetosphere, the plasma wave instrument detected electron plasma oscillations, upper hybrid resonance emissions, half-gyrofrequency harmonics, hiss and chorus, narrowband electromagnetic emissions and broadband Saturn radio noise, and noise bursts with characteristics of static. At the ring plane crossing, the plasma wave instrument also detected a large number of intense impulses that we interpret in terms of ring particle impacts on Voyager 2.*

The Voyager 1 and Voyager 2 trajectories through Saturn's magnetosphere were designed to differ in their distances of closest approach and ring plane crossing and directions of arrival and departure; information from Voyager 2 was expected to supplement and extend the earlier measurements by Voyager 1 (*1*) of plasma wave phenomena and wave-particle interactions. We have found that many of the August 1981 Voyager 2 wave observations, such as the measurements of electromagnetic hiss, chorus, narrowband emissions, and certain impulses in Saturn's inner magnetosphere, can be related to corresponding measurements obtained during the November 1980 Voyager 1 encounter. Other aspects of the Voyager 2 wave observations differed, however, especially during the outbound passage; these differences suggest the presence of effects associated with significant north-south or noon-dawn asymmetries, temporal variations associated with fluctuating solar wind conditions, or proximity to the Jupiter tail and wake (*2*). Another significant difference on Voyager 2 occurred at the close-in ring plane crossing ($R \approx 2.88\ R_S$), where the plasma wave instrument detected a large number of intense impulses that we interpret in terms of ring particle impacts on Voyager 2.

Magnetospheric size. One striking indication that Saturn's magnetosphere had changed by the time of the Voyager 2 encounter comes from comparison of the positions of the first and last crossings of the bow shock, which are marked in Fig. 1C. The dashed curves show the Voyager 1 trajectory and the nominal Voyager 1 bow shock surface in cylindrical coordinates, X versus $(Y^2 + Z^2)^{1/2}$; the heavy solid curve gives the corresponding Voyager 2 encounter trajectory. Figure 1, A and B, displays the plasma wave measurements for the first Voyager 2 inbound shock crossing [1337 spacecraft event time (SCET) on 24 August 1981, at 31.7 R_S, near local noon] and the last outbound crossing (0109 on 31 August 1981, at 87.4 R_S, near local dawn). It is noteworthy that these wave measurements are so similar, although the location of the final outbound crossing was about twice as far from Saturn as would be expected from scaling of the Voyager 1 shock surface out to intersect the Voyager 2 inbound crossing point.

The Voyager 2 plasma probe detected highly variable solar wind pressure before 24 August (*3*), and our measurements of intense upstream plasma oscillations at $f \approx 1.8$ kHz just before 1337 indicate that the local solar wind density (N) was near 0.04 particle per cubic centimeter just before this shock crossing. Since 3.1-kHz electron plasma oscillations (corresponding to $N \approx 0.11\ \text{cm}^{-3}$) were detected in a similar upstream location on Voyager 1 (*4*), the lower wind pressure at the Voyager 2 encounter seems to explain the somewhat bigger magnetosphere detected near local noon (with first shock crossing at 32 R_S rather than at 26 R_S). However, these simple density considerations do not seem able to account for the great distance to the

0036-8075/82/0129-0587$01.00/0

final outbound bow shock crossing, since Fig. 1B again shows 1.8-kHz electron plasma oscillations just beyond this crossing at 87 R_S. The problem persists even when a more complete analysis using the full solar wind pressure is carried out; Bridge *et al.* (*3*) noted that the pressures before the first inbound crossing and after the last outbound one were approximately equal.

It might seem that the Voyager 2 outbound observations could best be explained by assuming that the solar wind pressure was exceptionally low until just before the spacecraft emerged into the solar wind. In fact, low average pressures must have been present for an extended period because the outbound magnetopause was first traversed near 1640 on 28 August when Voyager 2 was at 48.5 R_S. There is also evidence for much variability about the average because there were many Voyager 2 shock crossings, covering the ranges 31.7 to 23.6 R_S (near noon) and 77.8 to 87.4 R_S (near dawn).

Very low plasma pressures would have developed if Jupiter's magnetic tail or the associated wake region had swept across Saturn's magnetosphere during the Voyager 2 encounter (*2*). Because the plasma wave and plasma probe investigators have jointly determined that Voyager 2 reentered Jupiter's tail as late as 17 to 19 July 1981, it is possible that Voyager 2 and Saturn could have been back in the tail or wake late in August. We will discuss the way in which the very low levels of radio emissions detected by the plasma wave instrument might also be explained in terms of encounter with Jupiter's tail or wake. However, we have so far found no direct evidence to support this conjecture.

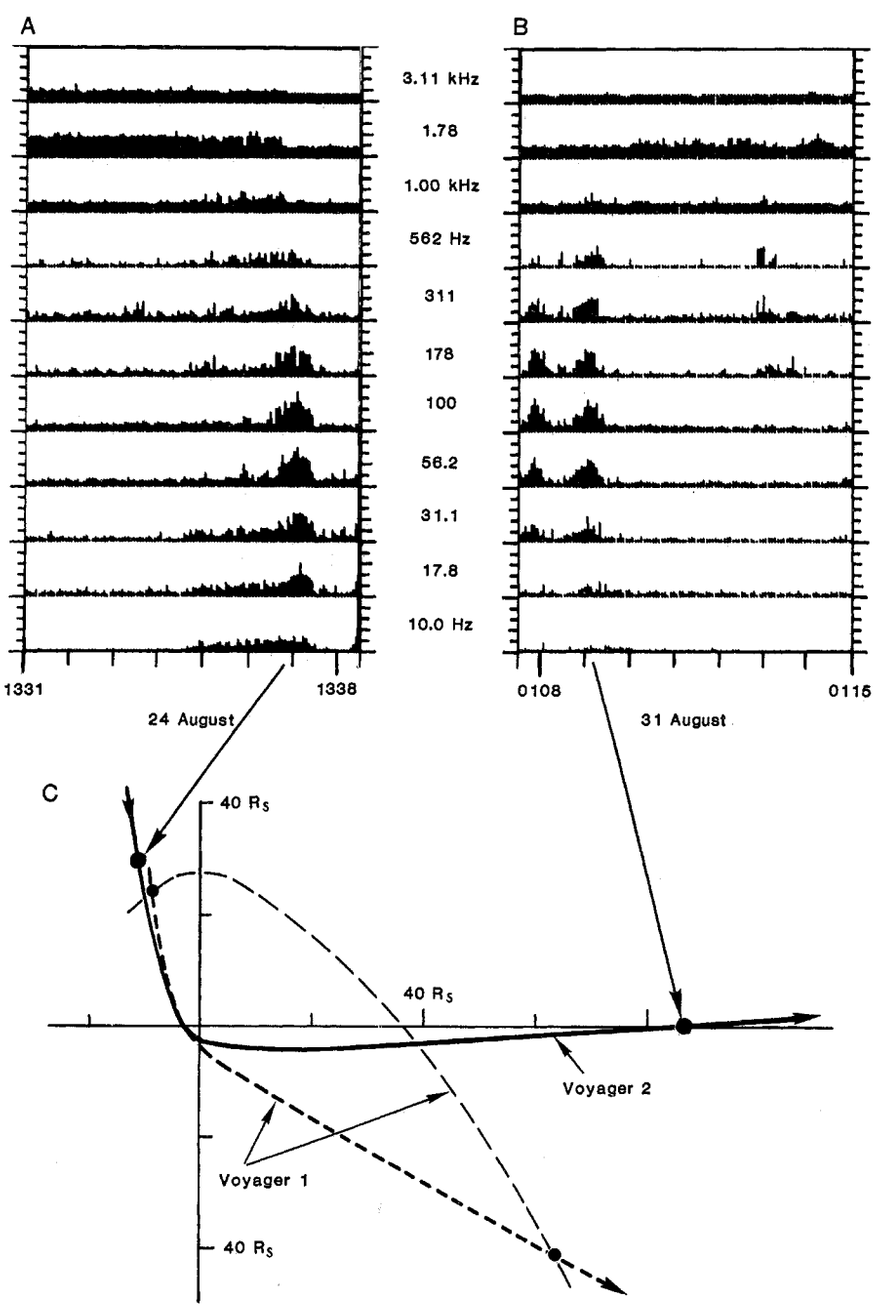

Fig. 1. (A and B) Plasma wave measurements for the first inbound (A) and last outbound (B) Voyager 2 crossings of the bow shock. (C) A nominal Voyager 1 bow shock surface plus trajectory plots for Voyager 1 (dashed lines) and Voyager 2 (solid line) in rotated coordinates [X versus $(Y^2 + Z^2)^{1/2}$].

The inner magnetosphere. The last inbound shock crossing occurred near 0030 on 25 August (at $R = 23.6\ R_S$), and Voyager 2 entered Saturn's magnetosphere just before 0700 ($R \approx 18.8\ R_S$). While the spacecraft was in the magnetosheath, strong radio emissions were detected almost continuously in the four channels extending from 10 to 56 kHz. Between 0650 and 0730, the 10-kHz level decreased and very weak 5.6-kHz signals were detected. If we assume that these 5.6-kHz waves represent electrostatic or electromagnetic waves similar to those observed just within the magnetopause at Earth and Jupiter (*5*), the sequence of measurements implies that $0.4 \lesssim N \lesssim 1$ electron per cubic centimeter in the magnetosheath before 0650, and $N < 0.4$ cm^{-3} in the outer magnetosphere.

All of the wave levels were extremely low when Voyager 2 was inbound beyond 12 R_S, but in the inner magnetosphere, the plasma wave instrument detected intense turbulence with rapid changes in the spectral characteristics. During the 24-hour period centered around closest approach (0320) and the ring plane crossing (0418), the 16-channel analyzer provided the customary full scan every 4 seconds; there were also 16 waveform frames, or 48-second opportunities to sample the antenna waveform at a rate of 28,800 measurements per second (*6*). Figure 2 contains relevant trajectory information for this 24-hour interval along with a summary of the 16-channel wave observations (96-second averages for the lower eight channels, and 96-second peaks and averages for the upper eight channels). The times for the waveform frames are indicated by the vertical bars and numbers just above the 16-channel data plot, and the profile of the electron cyclotron frequency, f_c, is drawn across the figure (f_c in hertz equals 28B where the magnetic field strength, B, is given in nanoteslas (*7*); 1 nT = 10^{-5} gauss).

The full analysis of the wave modes also requires knowledge of the electron

plasma frequency (f_p), which depends on the density (N) where N (in cubic centimeters) = $[f_p(\text{Hz})]^2/9000$. In some cases, the identification of an emission at f_p directly leads to an absolute sheath-independent evaluation of the ambient electron density (for example, the discussion of Fig. 1 and the plasma oscillations detected upstream from the bow shock). However, within a planetary magnetosphere, it is more common to be able to detect and identify the related emission at the upper hybrid resonance, f_{UHR}, where $f^2_{UHR} = (f^2_c + f^2_p)$. The direct measurement of f_{UHR} and the knowledge of f_c (from B-field observations) then leads to an evaluation of f_p and N.

The UHR emission is characteristically one of the most intense and impulsive magnetospheric signals observed in the spectral region above the electron cyclotron frequency. When the plasma density profile varies smoothly, it is frequently possible to follow this variation as the f_{UHR} emission moves from one narrowband filter channel to another. Figure 2 shows this behavior for the inbound pass; we identify the bursts detected at 5.6 kHz (1640 to 1700), at 10 kHz (2040 to 2120), and at 17.8 kHz (2235 to 2315) as UHR emissions, and we derive electron density estimates of 0.4 cm^{-3} near 10.5 R_S, 1.2 cm^{-3} near 7 R_S, and 3.9 cm^{-3} near 5.2 to 5.9 R_S (close to the Dione L shell). As Voyager 2 moved out past the Dione L shell on the outbound leg (0735 to 0810), intense 17.8-kHz emissions were again detected, suggesting a second encounter with a thin high-density region. No other noise bursts with clear characteristics of UHR emissions were detected after 0810.

In order to proceed with the discussion of the plasma wave observations in Saturn's inner magnetosphere, it is useful to compare some of the high-resolution information from the waveform frames with the continuous low-resolution output of the multichannel spectrum analyzer. Figure 3 shows color-coded frequency-time spectrograms made up from three frames recorded when Voyager 2 was at 5.1 R_S and 3.1 R_S (inbound) and at 4.0 R_S (outbound). These spectrograms were selected to show characteristics of some of the dominant modes that interact strongly with Saturn's plasma population and trapped energetic particles, and they also illustrate the detection of the strong noise bursts with characteristics of static.

Figure 3A shows an intense, structured, banded emission with $6.1 \lesssim f \lesssim 7.2$ kHz, a much weaker signal with $f \approx 8.8$ to 9.4 kHz, spacecraft interference tones at 100, 400, 1600, and 2400 Hz, and a large number of vertical striations. (Speculations on the origins of these impulsive noise bursts resembling static are contained in the final section on the ring plane crossing.) At 2325, the average field magnitude (*7*) was 220 nT; thus f_c was near 6.16 kHz, so that the frequency of the strong emission was just above f_c. This suggests that the wave is an electrostatic cyclotron harmonic mode of the type commonly called the "three-halves" wave. These oscillations frequently have $f \approx 3f_c/2$, but detection with f slightly higher than f_c is not uncommon (*8*), and the structured appearance of the signal almost exactly parallels the characteristics of corresponding emissions detected on Voyager 2 at the time of the closest approach to Jupiter (*9*). An intense cyclotron harmonic wave with $f \gtrsim f_c$ was also present in the preceding waveform frame (starting at 2323:59), and similar strong $3f_c/2$ waves appeared in the outbound frames with start times 0735:59, 0736:47 ($R \approx 5.2$ R_S), and 0858:23 ($R = 6.28$ R_S). Electrostatic cyclotron emissions were present throughout the inner magnetosphere, and this mode can be associated with the band of enhanced wave turbulence found in several narrowband channels just above the f_c profile (Fig. 3). At Earth, the $(n + 1/2)f_c$ emissions cause electron precipitation into the atmosphere, producing the diffuse aurora (*10*); we expect that similar phenomena are present at Saturn.

Figure 3B shows a broad low-frequency hiss band ($0.5 \lesssim f \lesssim 1.8$ kHz), an intense intermittent emission at $f = 2.7$ kHz, and a much weaker band centered at $f \approx 3.25$ kHz. At this time, f_c was 25.5 kHz, and we associate the 2.7-kHz waves with f_p (on the basis of plasma probe data) and infer the presence of a field-aligned electron beam. This identification of f_p suggests that the hiss band is whistler-mode turbulence and that the weak 3.25-kHz waves represent electromagnetic radiation. The whistler-mode waves produce electron pitch-angle diffusion and atmospheric precipitation, but for this low plasma density and high magnetic field strength, the hiss band at 0200 interacts resonantly with energetic electrons (in the range 6 to 20 MeV), and, thus, this precipitation does not lead to an auroral emission.

Figure 3C again shows a hiss band ($f \approx 0.8$ to 1.3 kHz) and a structured

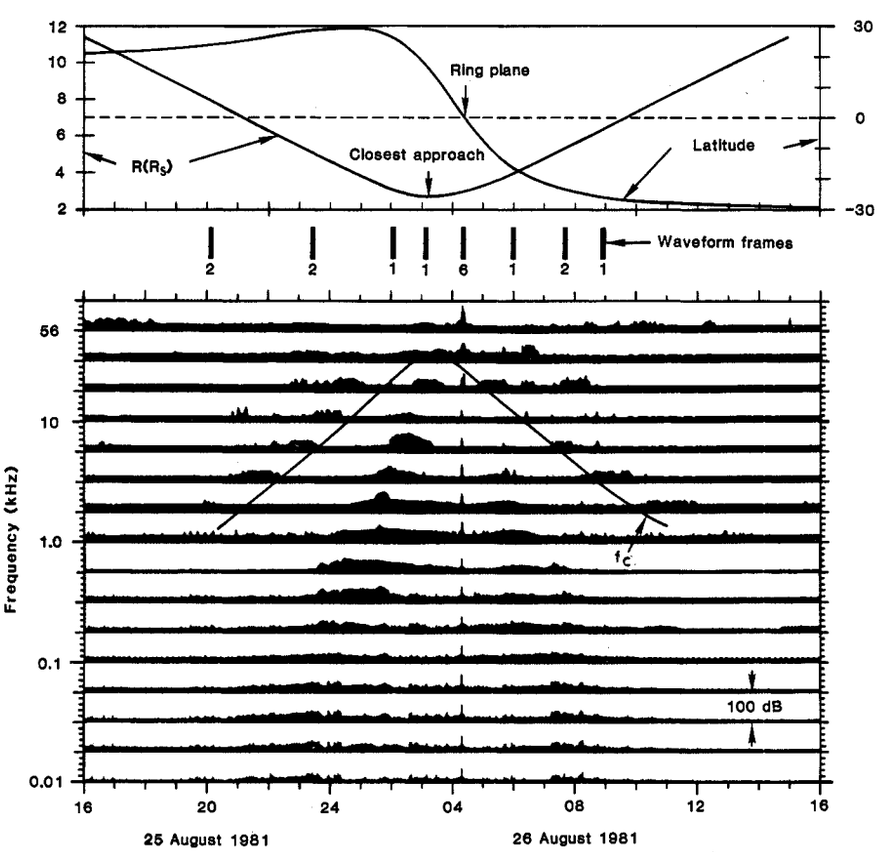

Fig. 2. Summary plot of the 16-channel spectrum analyzer measurements near closest approach. The electron cyclotron frequency is f_c, and the bars and numbers between the data plot and the trajectory panel give the location and the number of the 48-second waveform frames.

higher frequency emission ($f \approx 2.8$ to 3.5 kHz) that we identify as chorus. (This Voyager 2 chorus structure resembles that detected on Voyager 1 as the spacecraft approached the magnetic equator near 5.4 R_S.) At 0600 on 26 August, the Voyager 2 magnetometer data gave $f_c = 10.9$ kHz and the plasma probe observations gave $f_p = 2.8$ kHz. Once again, we find that (f_c/f_p) was large, leading to very high resonant energies; the hiss band would scatter electrons with $E \approx 2.8$ to 4.4 MeV, while the chorus would interact with electrons having $E \approx 950$ keV to 1.3 MeV. Thus, it appears that none of the Voyager 2 measurements of whistler-mode turbulence involved waves that could interact locally with electrons having low enough energy to produce auroral emissions in the visible or ultraviolet range. However, Voyager 2 was generally in a low-density region, and the corresponding chorus detected on Voyager 1 nearer to the equatorial plasma disk did interact with electrons of much lower energy.

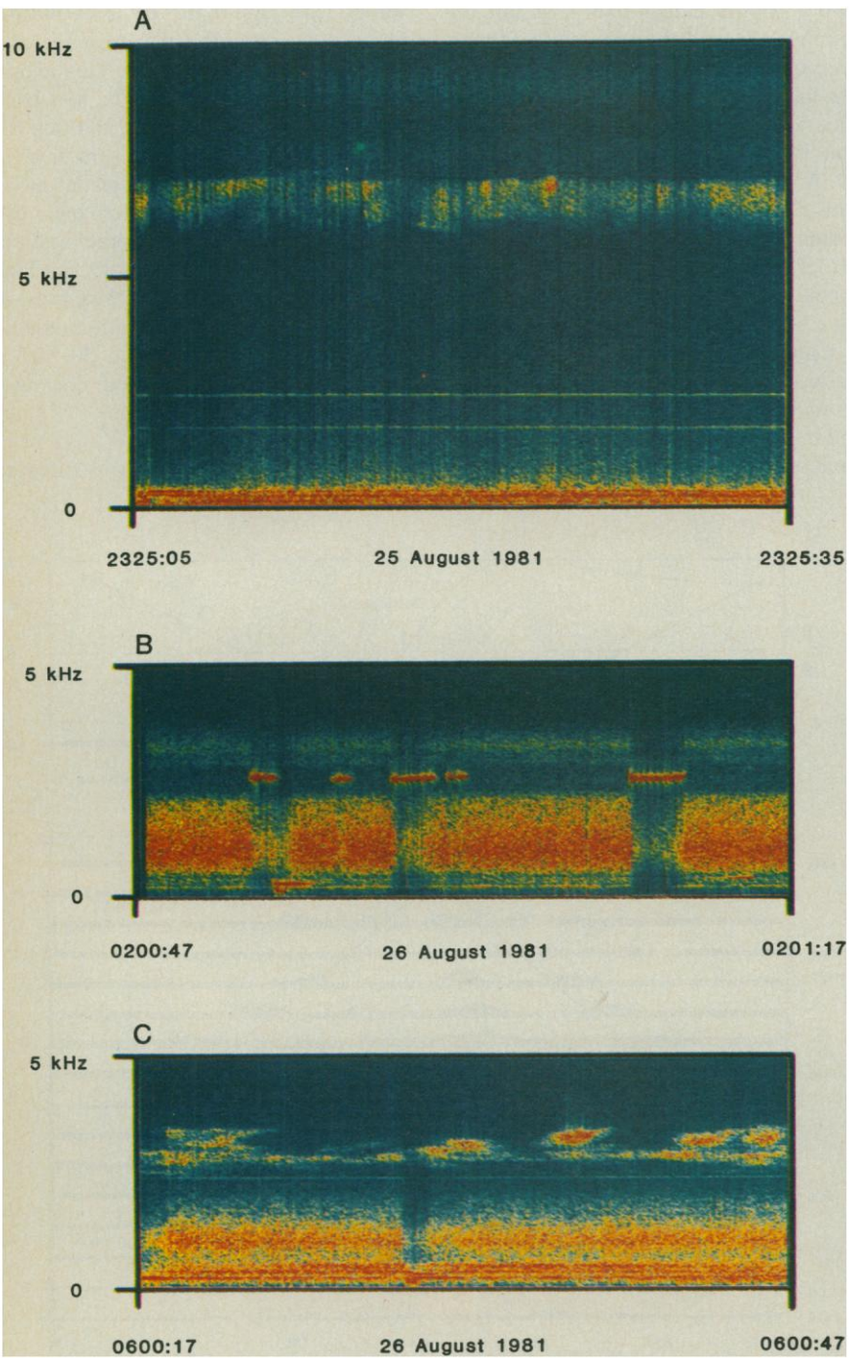

Fig. 3. Color-coded spectrograms showing (A) an electrostatic cyclotron harmonic emission, (B) hiss and electron plasma oscillations, and (C) hiss and chorus. For these three panels, the radial distances and electron cyclotron frequencies are (A) $R = 5.1\ R_S$, $f_c = 6.16$ kHz; (B) $R = 3.1\ R_S$, $f_c = 25.5$ kHz; and (C) $R = 4.0\ R_S$, $f_c = 10.9$ kHz. The color coding has red for the strongest signals and blue for the weakest.

Low-frequency radio waves. The waveform frame that started at 0200:47 (Fig. 3) contained no high-frequency ($f > 4$ kHz) wave activity other than weak bursts at $2f_p$ that contain harmonic distortion from the intense signals at the electron plasma frequency. However, 78 seconds after this frame ended, the amplitude in the 5.6-kHz spectrum analyzer channel, which had been at background, rose abruptly by more than an order of magnitude. The 5.6-kHz level peaked between 0210 and 0235, and the amplitude then decreased to background between 0315 and 0320 (closest approach) (Fig. 2). In the midst of this period, we again had a waveform frame (Fig. 4A). For comparison, Fig. 4B shows a portion of a Voyager 1 wideband frame containing a large number of intense narrowband emissions. Figure 4 demonstrates that the high-frequency signal detected on Voyager 2 was an intense narrowband tone at 6 kHz and that essentially the same 6-kHz signal was detected 9 months earlier, shortly before the closest approach of Voyager 1.

There are many more lines on Fig. 4B than on Fig. 4A, but in both cases we also find a broad hiss band below 2 kHz and a weak but diffuse narrowband emission at $f \approx 8.2$ to 8.5 kHz. The weak 3.25-kHz band detected 1 hour earlier on Voyager 2 (Fig. 3B) also corresponds to one of the narrow Voyager 1 lines from Fig. 4, which suggests a surprising persistence in these unique but apparently characteristic emissions from Saturn's inner magnetosphere.

Gurnett *et al.* (*1, 11*) interpreted the Voyager 1 observations in terms of electromagnetic waves propagating in the free-space left-hand polarized ordinary (L, 0) mode, and they proposed a generation model involving conversion of electrostatic emissions to electromagnetic radiation in regions where steep density gradients occur and where $f_{UHR} = (n + 1/2)f_c$. The Voyager 2 data appear consistent with this concept, although Gurnett *et al.* (*1, 11*) associated specific pairs of emissions with the cyclotron frequency at the source region, and their Voyager 1 model placed the source of the main 6-kHz emission at a radius of 5.4 R_S rather than just within 3.1 R_S (0200) where Voyager 2 first detected these waves. The Voyager 2 data also introduce the possibility that the origin of the emission might involve f_p rather than the other electrostatic modes.

Another prominent difference between the two data sets involves the range of detectability of the 6-kHz emission. Figure 5 contains meridian-plane trajectory projections for both Voyager encounters. The black Voyager 1 box shows the spacecraft location at 2252, whereas the corresponding Voyager 2 black segment covers the entire passage from 0200 to 0320. The open boxes indicate where weaker emissions were observed. As noted by Gurnett *et al.* (*11*), the 6-kHz tone was sporadically detected to almost 60 R_S during the Voyager 1 outbound pass, but the only other Voyager 2 waveform frame with evidence for a narrowband emission is Fig. 3B, which contains the very weak signal at $f \approx 8.8$ to 9.4 kHz.

The fact that no narrowband emissions were detected during the Voyager 1 inbound pass is understandable because the spacecraft remained close to the high density ($f_p > 6$ kHz) equatorial plasma disk. It is also possible that on Voyager 2 the thin region of high density near the Dione L shell simply blocked the radiation from the spacecraft when $R > 5.4$ R_S, as indicated by the portions of the trajectory beyond the region marked by line segments in Fig. 5. The great difference in the Voyager 1 and Voyager 2 detection of these narrowband signals during the outbound passes suggests, however, that additional radio emission phenomena should be examined for evidence of possible asymmetries or temporal variations.

The local characteristic frequencies f_c, $(n + 1/2)f_c$, and f_{UHR} are all below 10 kHz beyond about 10 to 12 R_S, so that the 10- to 56-kHz channels of the Voyager plasma wave investigations provide a capability for study of the low end of Saturn's kilometric radio spectrum in the outer magnetosphere and solar wind. Figure 6 shows the relevant four-channel 16-day amplitude plots centered around the closest approach times. The vertical lines mark the ring plane or magnetic equator crossings, and all of the signals except for those in the inner region (parts of 12 and 13 November 1980 and 25 and 26 August 1981) are identified as Saturn radio emissions. The Voyager 1 observations show many bursts with peaks separated by the Saturn magnetic rotation period (10 hours, 39.4 minutes), but there is also evidence for much irregularity, some of which has been attributed to Dione's modulation effect (*1, 12*). On Voyager 1, this irregularity was limited in the sense that there were no intervals longer than 24 hours without detectable low-frequency Saturn radio emissions during the time that the spacecraft was within 180 to 200 R_S. The upper panel in Fig. 6 shows that the situation was extremely different during the Voyager 2 outbound pass; from 1200 on 26 August ($R = 9$ R_S) until about 1200 on 31 August ($R = 95$ R_S) there were no strong emissions in any of the 10- to 56-kHz channels; with the exception of some weak noise bursts on 29 August, one could almost conclude that Saturn turned off as a low-frequency radio emitter for more than 4 days.

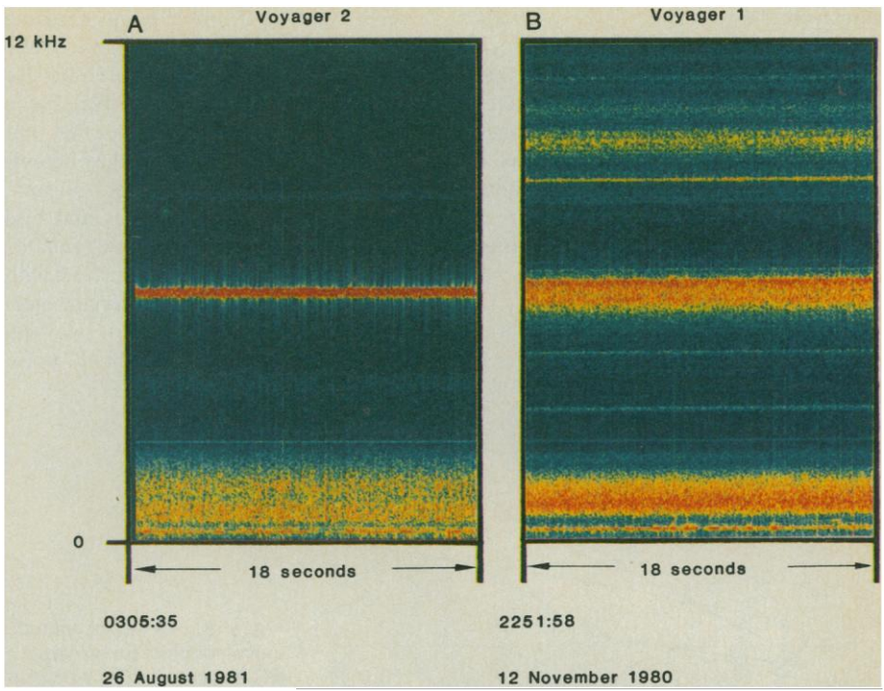

Fig. 4. Comparison of Voyager 1 and Voyager 2 detection of hiss (bottom) and narrowband emissions in the inner magnetosphere. (A) Data taken when the spacecraft was at $R = 2.7$ R_S, 17° north latitude. (B) Data taken when the spacecraft was at $R = 3.26$ R_S, 40° south latitude.

The labels above the data panels in Fig. 6 suggest that these differences might arise because Voyager 2 left Saturn south of the equator and ring plane, whereas the Voyager 1 outbound pass and both approaches were in the north. Kaiser *et al.* (*13*) have suggested that the source region for the kilometric radio emissions detected by Voyager 1 is near the noon meridian in the northern auroral zone, the polar cusp, or both, although the spacecraft spent only 20 hours in the southern hemisphere, and the Dione modulation effect complicated the analysis. On the other hand, examination of the plasma wave data to 21 September tends to support an explanation involving a north-south asymmetry in the radio emission pattern; although strong bursts were detected on 31 August, no other intense radio signals with $f \lesssim 56$ kHz were observed during the next 3 weeks.

An objection to this interpretation arises because we did, in fact, detect weak radio emissions in the south on 29 August and strong ones on 31 August. These events occurred soon after the outbound crossings of the magnetopause and the sequence of bow shocks. If these radio emissions originate in the polar cusp (*13*), changes in solar wind pressure should directly affect the radiation, so that the low pressure associated with the unusually long outbound magnetosphere pass would naturally be accompanied by low levels of radio emission. Indeed, if Saturn had reentered the Jupiter tail or wake between 26 August and 31 August, we would expect to find an enlarged magnetosphere together with an absence of radio emissions, as we did.

The ring plane crossing. When Voyager 1 crossed the ring plane and magnetic equator near the Dione L shell, the plasma wave instrument detected a broad intensity peak in the whistler-mode turbulence and in the $(n + 1/2)f_c$ bands (*1*) (Fig. 3). About 45 minutes earlier, a Voyager 1 waveform frame confirmed the presence of strong chorus and whistler-mode hiss and weaker cyclotron harmonic emissions, together with a large number of intense impulsive noise bursts that were clearly detectable only in the wideband data [Fig. 5B in (*1*)]. In commenting on the sounds derived from the "static" or impulses which accompanied the chorus, Scarf *et al.* suggested possi-

ble interpretations involving "(a) lightning from the atmosphere, (b) discharges from the spacecraft, dust, and/or ring material, (c) impacts on the spacecraft, (d) Doppler-shifted ion acoustic waves" (*14*, p. 2). We anticipated that Voyager 2 would provide much more definitive information, and arrangements were made to record six waveform frames in the equatorial region, including one frame that would contain data taken during the actual ring plane crossing.

Figure 2 shows that fairly low wave levels were detected throughout the region near Voyager 2 closest approach except right at the ring plane crossing (0418). The Voyager 2 plasma probe reported a very low plasma density ($N \ll 0.1$ cm^{-3} or $f_p \ll 2.8$ kHz) for a period of hours around this time, but within 0.4 R_S of the equator, they detected a high density of very cold plasma. The absence of strong chorus and hiss near the Voyager 2 magnetic equator crossing is likely to be associated with the fact that the fluxes of resonant electrons were very low (*3, 15*); we will consider the intense broadband noise bursts detected in the immediate vicinity of the ring plane.

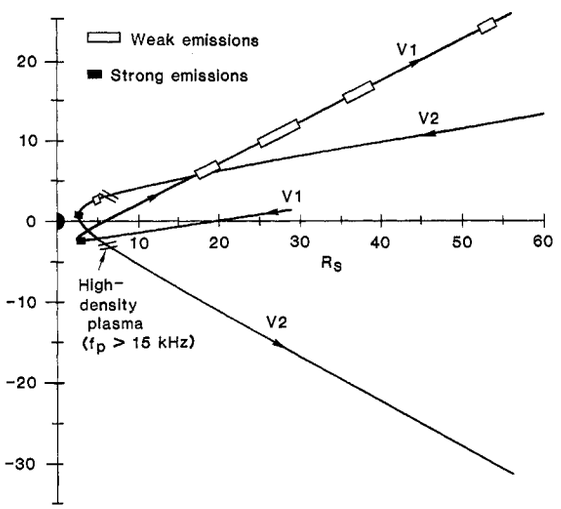

Fig. 5. Radius versus latitude trajectory plots for Voyager 1 and Voyager 2. The boxes indicate where narrowband electromagnetic emissions were detected.

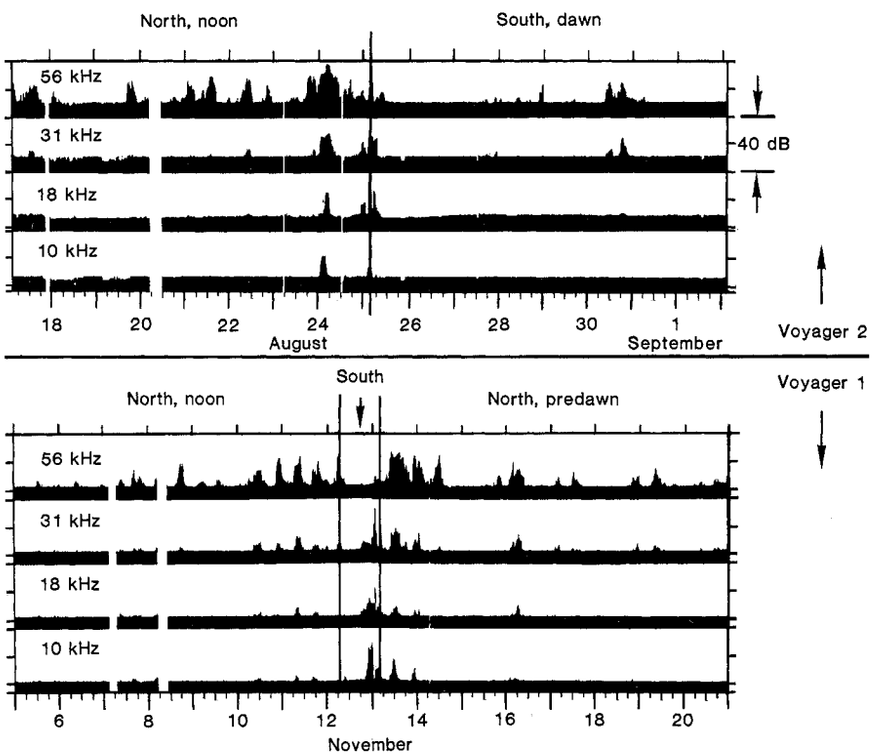

Fig. 6. Comparison of high-frequency plasma wave measurements for Voyager 1 and Voyager 2. The 16-day plots are centered around closest approach, where some of the measurements represent local plasma waves. With the exception of data from 25 and 26 August and 12 and 13 November, all of these signals represent Saturn radio emissions.

Figure 7A shows an expanded meridian plane plot of the Voyager 2 trajectory near closest approach. The heavy segment emphasizes the interval from 0405 to 0430; the time axis of the 16-channel spectrum analyzer plot for this interval is vertical (Fig. 7B), in accordance with the actual spacecraft motion from north to south. This shows that with the exception of an extremely intense and brief broadband noise burst centered at the ring plane crossing, the wave levels below 30 kHz were almost at background for 25 minutes as Voyager 2 moved from 9050 km above the ring plane to 7800 km below the plane. The central noise burst, which almost saturated the plasma wave receiver, lasted for approximately 2 or 3 minutes, corresponding to a north-south extent ± 700 to 1000 km, which is about equal to the anticipated thickness of an outer ring system such as the E ring or the G ring (*16*).

It is not possible to explain the intense noise burst of Fig. 7 in terms of external plasma wave phenomena. At 0418, f_c was above 25 kHz, but the noise spectrum extended smoothly across this characteristic plasma frequency, suggesting that electrical impulses associated with local phenomena on the spacecraft were detected. [The moderate radio noise or 3 $f_c/2$ emission in the 31- and 56-kHz channels of Fig. 7 may obscure the fact that the ring plane noise spectrum extends above f_c, but this peak was still detected in these high-frequency channels. Moreover, the planetary radio astronomy receiver on Voyager 2 observed strong signals to much higher frequencies (*17*), and the combined spectrum verifies that the ring plane noise has no resonances or cutoffs at the local characteristic plasma frequencies.]

Unambiguous identification of this noise phenomenon comes from analysis of the waveform data. Figure 8B shows the calibrated 56-Hz electric field amplitude plot along with marks indicating the locations of the six waveform frames. The ring plane was crossed during the last part of the wideband frame that went from 0417:35 to 0418:23. At this time we also detected the highest E field reading since launch in the 56-Hz channel [E (peak) ≈ 1000 times the "ambient" value].

The sound recording derived from this waveform frame provides a convincing way to identify the source of the intense turbulence. We summarize the audio analysis by stating that the sounds, which resemble a hailstorm, are those of impacts on the spacecraft. Further clari-

fication comes from examining the highest-resolution electric-field time profile. The inset in Fig. 8A shows an E field plot with 35 μsec between samples. This figure shows that the ring plane crossing noise consists of a sequence of short ($\tau \approx$ milliseconds or less) impulses. Since the relative velocity between the orbiting ring material and Voyager 2 exceeded 14 km/sec at this point, any dust particles impacting the spacecraft would break up into ionized fragments (*18*). We propose that the observed signals are electrical impulses associated with charged dust particles, and we note that the peak impact rate was greater than 200 per second. Since ground-based observations show that particles in the G and E rings are in the range 5 μm or less (*19*), the total particle mass flux was low even though the impact rate was high.

The ring plane spectral density (Fig. 8A) is preliminary and subject to correction because it includes effects of impulses that are strong enough to be clipped by the waveform receiver. A preliminary power spectrum made up from only unclipped impulses is flatter below 100 to 200 Hz, and it falls off less steeply than the $\approx (f)^{-2.5}$ behavior shown here. However, the spectrum in Fig. 8 is correct in the sense that it demonstrates how the ring plane noise is peaked below 100 to 200 Hz, consistent with a maximum impact rate of hundreds of hits per second. We conclude that Voyager 2 actually passed through an extension of Saturn's G ring and that the ring material hit the spacecraft, producing the noise characteristics of Figs. 7 and 8.

Although these conclusions are derived from analysis of audio frequency waves, our techniques do not have the ambiguity associated with early microphone dust-detector systems in which thermal creaks were counted as dust impacts; on Voyager, creaks, thruster firings, and other spacecraft noises are frequently detected, but they have recognizable frequency spectra and characteristic intensity levels and repetition rates different from the ones shown in Figs. 7 and 8. It is also significant that the Voyager plasma wave instrument found no detectable changes in wave level or noise bursts associated with passage into Saturn's shadow at 0409 (Fig. 7) and we conclude that there were no detectable thermal creaks as the spacecraft temperature stabilized in shadow.

The waveform frames extending out to 0425 had a relatively small number of impulses, and the audio analysis suggests the characteristics of "static" (Fig. 3A) rather than the "hailstorm" effect associated with the sounds from the ring plane crossing frame. This distinction is similar to one derived from the Voyager 1 waveform data, in which the frame nearest the ring plane crossing (at 5.4 R_S) had sounds suggesting impacts, whereas static sounds appeared on the frames recorded on 12 November 1980 at 0143 (24 R_S), 1257 (12.5 R_S), and 1830 (6.9 R_S), and on 13 November at 0108 (3.6 R_S) (*14*). However, high-resolution analysis of the E waveform amplitude data shows that the static sounds come from undispersed or local impulses associated with $E(t)$ profiles essentially identical to the one contained in the inset of Fig. 8A. This result suggests that dust impacts cause impulses even at locations

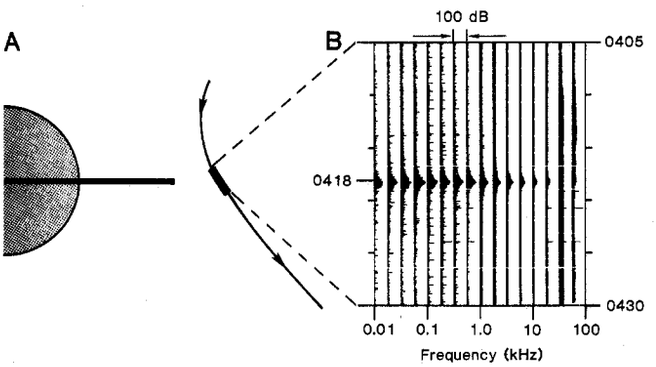

Fig. 7. (A) Voyager 2 trajectory (radius versus latitude). (B) Expanded plot of the 16-channel spectrum analyzer data for the 25-minute interval centered around the ring plane crossing.

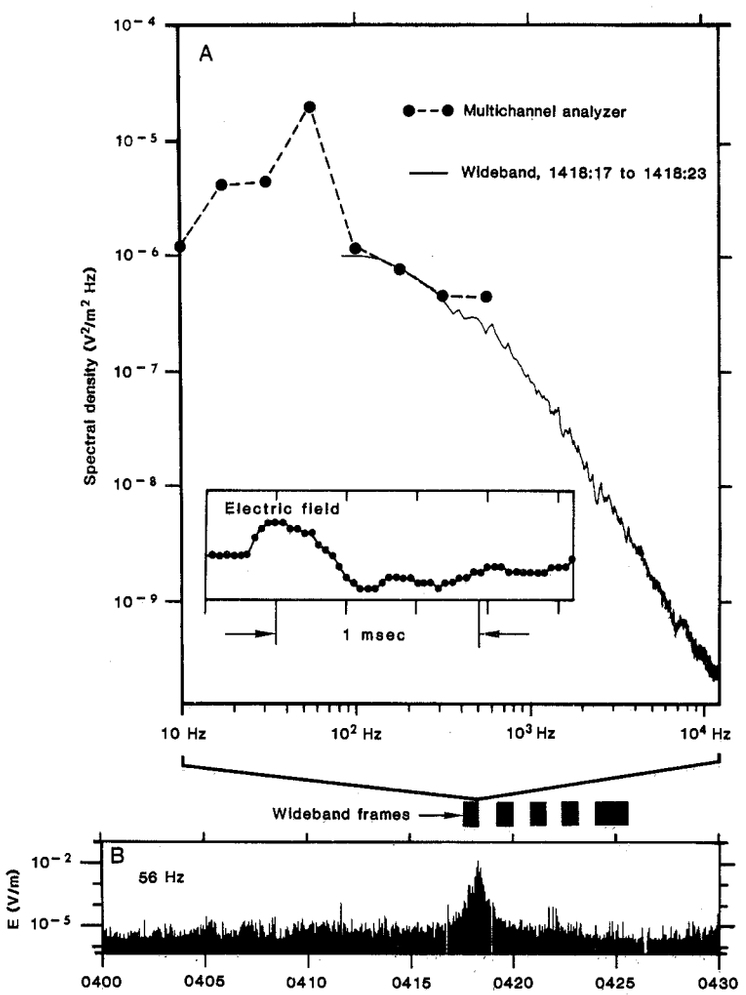

Fig. 8. (A) Plasma wave spectral density (uncorrected for clipping or saturation effects) associated with the peak turbulence detected as Voyager 2 crossed the ring plane. (Inset) A high-resolution $E(t)$ profile showing the impulse associated with one (typical) impact at the ring plane crossing. (B) Display of the 56-Hz amplitude profile along with the positions of six waveform frames recorded at and near the ring plane crossing.

far from the rings, and it may mean that Saturn's gravity attracts dust over very large distances. Similar impulses have never been detected when Voyager 2 was in cruise, and they are not clearly evident in the Jupiter data analyzed to date; our initial analysis of Jupiter wave observations concentrated on frames having intense plasma wave activity, however, and weak bursts of undispersed impulsive noise would not appear.

F. L. SCARF

Space Sciences Department,
TRW Defense & Space Systems Group,
Redondo Beach, California 90278

D. A. GURNETT, W. S. KURTH

Department of Physics and Astronomy,
University of Iowa, Iowa City 52242

R. L. POYNTER

Jet Propulsion Laboratory,
California Institute of Technology,
Pasadena 91109

References and Notes

1. D. A. Gurnett, W. S. Kurth, F. L. Scarf, *Science* **212**, 235 (1981).
2. F. L. Scarf, *J. Geophys. Res.* **84**, 4422 (1979); _____, W. S. Kurth, D. A. Gurnett, H. S. Bridge, J. D. Sullivan, *Nature (London)* **292**, 585 (1981).
3. H. S. Bridge *et al.*, *Science* **215**, 563 (1982).
4. F. L. Scarf, D. A. Gurnett, W. S. Kurth, *Nature (London)* **292**, 747 (1981).
5. D. A. Gurnett and R. R. Shaw, *J. Geophys. Res.* **78**, 8136 (1973); F. L. Scarf, D. A. Gurnett, W. S. Kurth, *Science* **204**, 991 (1979); D. A. Gurnett, W. S. Kurth, F. L. Scarf, *ibid.* **206**, 987 (1979).
6. F. L. Scarf and D. A. Gurnett, *Space Sci. Rev.* **21**, 289 (1977).
7. N. F. Ness *et al.*, *Science* **215**, 558 (1982).
8. C. F. Kennel, F. L. Scarf, R. W. Fredricks, J. H. McGehee, F. V. Coroniti, *J. Geophys. Res.* **75**, 6136 (1970).
9. W. S. Kurth, D. D. Barbosa, D. A. Gurnett, F. L. Scarf, *Geophys. Res. Lett.* **7**, 57 (1980).
10. L. R. Lyons, *J. Geophys. Res.* **79**, 575 (1974).
11. D. A. Gurnett, W. S. Kurth, F. L. Scarf, *Nature (London)* **292**, 733 (1981).
12. W. S. Kurth, D. A. Gurnett, F. L. Scarf, *ibid.*, p. 742; M. D. Desch and M. L. Kaiser, *ibid.*, p. 739.
13. M. L. Kaiser, M. D. Desch, A. Lecacheux, *ibid.*, p. 731.
14. F. L. Scarf, D. A. Gurnett, W. S. Kurth, *TRW Tech. Report 23498-6041-UT-00* (26 January 1981).
15. S. M. Krimigis *et al.*, *Science* **215**, 571 (1982).
16. D. H. Humes, R. L. O'Neal, W. H. Kinard, J. M. Alvarez, *ibid.*, **207**, 443 (1980).
17. J. Warwick *et al.*, *Science* **215**, 582 (1982).
18. E. Grün, in *Comet Halley Probe Plasma Environment* (European Space Technology Centre Publ. ESA SP-155, Noordwijk, 1981), p. 18.
19. R. J. Terrile and A. Tokunaga, *Bull. Am. Astron. Soc.* **12**, 701 (1980).
20. We thank the entire Voyager team at NASA Headquarters and the Jet Propulsion Laboratory (JPL) for their support. We are especially grateful to E. Miner and J. Diner for their efforts to arrange the wideband coverage at Saturn, and we thank J. Anderson, P. Jepson, and the staff at the Mission Test and Imaging Systems Laboratory and the Imaging Processing Laboratory for their assistance with the wideband data processing. We acknowledge with gratitude the continuous support from C. Stembridge, and we thank H. Bridge, J. Sullivan, J. Scudder, N. Ness, T. Krimigis, J. Warwick, J. Romig, M. Kaiser, and J. Alexander for providing data in advance of publication and for their helpful discussions. We are grateful to A. Cowen, S. Chang, and R. Tsugawa of TRW and R. Anderson, R. West, L. Granroth, and R. Brechwald of the University of Iowa for carrying out the data reduction. The research at TRW was supported by NASA through contract 954012 with JPL. The research at the University of Iowa was supported by NASA through contract 954013 with JPL, through grants NGL-16-001-002 and NGL-16-001-043 from NASA headquarters, and by the Office of Naval Research.

10 November 1981